

Investigation of Simple Shape Descriptors for NACA 4 Digit Airfoils

Haydar TUNA^{1*}, Ozcan YIRTICI²

^{1,2}Osmaniye Korkut Ata Üniversitesi, Mühendislik ve Doğa Bilimleri Fakültesi, Bilgisayar Mühendisliği Bölümü, 80000, Osmaniye, Türkiye

(Alınış / Received: 19.10.2024, Kabul / Accepted: 14.12.2024, Online Yayınlanma / Published Online: 23.12.2024)

Keywords

Shape representation,
Image processing,
Airfoil

Abstract: This study aims to define new simple shape descriptors to analyze airfoils. The ImageJ platform is used to calculate twelve different shape descriptors such as area, convex hull, contour temperature and solidity by performing image processing. One of the most important findings is that an increase in the thickness of an airfoil leads to corresponding increases in its area, perimeter, area of minimum enclosing area, and convex hull area. Another noteworthy discovery is that the values derived from these basic features, either increasing or decreasing. Simple shape features in the study are not used independently, as they do not possess distinct characteristics that set them apart from one another. Machine learning and deep learning applications can achieve greater success when these features are combined with other elements. The combination of these features with other shape attributes, such as chain code histograms, shape signatures, and central moments, can enhance the success of machine learning and deep learning applications.

NACA 4 Kanat Profillerinin Basit Şekil Temsil Yöntemleriyle İncelenmesi

Anahtar Kelimeler

Şekil temsili,
Görüntü işleme,
Kanat profili

Öz: Bu çalışma, kanat profillerini analiz etmek için yeni basit şekil belirteçlerini tanımlamayı amaçlamaktadır. ImageJ platformu, görüntü işleme gerçekleştirerek alan, dışbükey gövde, kontur sıcaklığı ve katılık gibi on iki farklı şekil tanımlayıcısını hesaplamak için kullanılır. En önemli bulgulardan biri, bir kanat profilinin kalınlığındaki artışın, alanında, çevresinde, minimum çevreleyen alan alanında ve dışbükey gövde alanında karşılık gelen artışlara yol açmasıdır. Dikkat çekici bir diğer keşif ise, bu temel özelliklerden türetilen değerlerin artması veya azalmasıdır. Çalışmada basit şekil özellikleri, onları birbirinden ayıran belirgin özelliklere sahip olmadıkları için bağımsız olarak kullanılmamaktadır. Makine öğrenimi ve derin öğrenme uygulamaları, bu özellikler diğer öğelerle birleştirildiğinde daha büyük başarı elde edebilir. Bu özelliklerin zincir kod histogramları, şekil imzaları ve merkezi momentler gibi diğer şekil nitelikleriyle birleştirilmesi, makine öğrenimi ve derin öğrenme uygulamalarının başarısını artırabilir.

1. Introduction

Aerodynamic design and optimization is still an important research area in Aerospace and Wind energy. Recently, artificial Intelligence has been used to predict aerodynamic loads at the conceptual design stage [1-3]. For this purpose, airfoil shape descriptors with a prediction methodology and sufficiently large aerodynamic dataset are required.

An airfoil is a closed defining shape for the wings and turbine blades to create a lift force. The thickness,

camber, curvature, and leading-edge radius have been investigated as shape descriptors that affect aerodynamic loads (lift, drag, and pitching moment) [4-6]. In recent studies, various machine learning methods have been employed to predict drag and lift coefficients. For example, artificial neural networks have been used to calculate these variables [7]. Zhang et al. applied Convolutional Neural Networks to transform airfoil shape images into discrete, ordered vector representations. These representations were subsequently utilized to train models for predicting

*Corresponding Author: haydartuna@osmaniye.edu.tr

aerodynamic parameters, including drag and lift coefficients [8].

There have not been extensive investigations on the use of simple shape descriptors for analyzing airfoils. This study aims to address this gap by assessing nine distinct shape descriptors on a dataset consisting of 120 airfoils across 20 families, each comprising six airfoils.

2. Simple Shape Descriptors

Simple shape descriptors or scalar values are commonly used to describe the geometric characteristics of shapes. The quantitative characteristics provided by these descriptors facilitate analysis and comparison. Although these descriptors may be useful in certain contexts, they are not sufficient for definitive shape characterization. These techniques are often augmented with other methods to increase their effectiveness [9]. Various descriptors, such as area, perimeter, minimum enclosed rectangular area, extent, and circularity, are typical examples of these descriptors.

2.1. Area

The most direct method for quantifying the area of an object is to enumerate the number of pixels that constitute a given shape. In a binary image, where pixels denoted as $\text{pix}(x,y)=1$ represent shape elements, and $\text{pix}(x,y)=0$ indicates background elements, the subsequent algorithm can be employed to approximate the area of an object.

Algorithm 1: Area Estimation of a Shape

```

1:  $area \leftarrow 0$ ;
2: for  $x \leftarrow 0$  to  $M-1$  do
3:   for  $y \leftarrow 0$  to  $N-1$  do
4:      $area \leftarrow area + \text{pix}(x, y)$ ;

```

where M and N denote the number of rows and columns, respectively. Furthermore, x represents the row index, and y represents the column index. This algorithm can be used to calculate the areas of the airfoils that have been scaled and converted into black-white images. For example, Figure 1 shows the areas of some 12XX family NACA airfoils. In this section, we select airfoils from the NACA-12XX family with 1000 points.

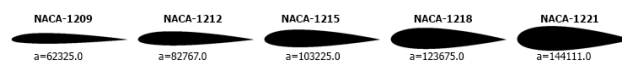


Figure 1. NACA-12XX family airfoils and their areas

2.2. Perimeter

Measurement of the perimeter of a shape involves calculating the distance between consecutive points on its contour. A viable solution to this problem is to

approximate the arc length using contour-based representation. This can be achieved by estimating the length of the arc based on the 4-neighborhood (FR4) and 8-neighborhood chain codes (FR8) used to represent the contour [10-11], as illustrated in Figure 2a and 2b.



Figure 2. Direction number of chain codes for a)FR4 b)FR8

The diagonal arc length was not considered when employing the FR4 chain code to determine perimeter. Thus, the FR4 chain code is unsuitable for calculating the perimeter. By contrast, when the FR8 chain code is employed to represent the contour, the arc length can be estimated as follows[12]:

$$p = n_e + n_o\sqrt{2} \tag{1}$$

where n_e represents the number of consecutive contour points with even direction codes, and n_o represents the number of odd-direction codes. Using this formula, the NACA-12XX family of airfoils and their corresponding perimeters were calculated, as shown in Figure 3.

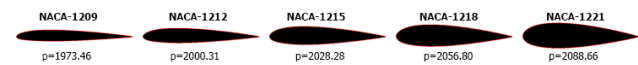


Figure 3. NACA-12XX family airfoils and their perimeters

2.3. Area-to-Perimeter ratio

The area-to-perimeter ratio is another fundamental shape descriptor, and its value is calculated using Equation 2 [9]. Figure 4 illustrates the area-to-perimeter ratio of sample airfoils from the NACA-12XX family.

$$apr = \frac{a_s}{p_s} \tag{2}$$

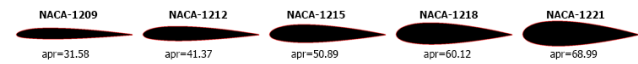


Figure 4. NACA-12XX family airfoils and area-to-perimeter ratios

2.4. Area of minimum enclosing rectangle

The area of the minimum enclosing rectangle (AMER) is defined as a rectangle whose sides lie on the x - y plane and enclose the shape with the least possible area. The use of a rotating caliper algorithm is recommended for determining the AMER. The same approach can be employed to identify the minimum perimeter enclosing a rectangle [13-15]. However, because the airfoils are parallel to the xy -plane and are not rotated, the following bounding box algorithm can be applied to determine the AMER:

Algorithm 2: Finding MER for Airfoil with bounding box algorithm

```

1:  xMin = M
2:  xMax = 0
3:  yMin = N
4:  yMax = 0
5:  for x ← 0 to M-1 do
6:    for y ← 0 to N-1 do
7:      if p(x,y)=1 and x < xMin then
8:        xMin = x
9:
10:     if p(x,y)=1 and x > xMax then
11:       xMax = x
12:
13:     if p(x,y)=1 and y < yMin then
14:       yMin = y
15:
16:     if p(x,y)=1 and y > yMax then
17:       yMax = y

```

where M is the width, and N is the height of the picture. $xMin$ and $xMax$ are the minimum and maximum x -coordinates on the shape. Similarly, $yMin$ and $yMax$ are the minimum and maximum y -coordinates, respectively, of the shape. Using this algorithm, the upper-left coordinates of the rectangle are determined as $(xMin, yMin)$ and the bottom-right coordinates of the rectangle are determined as $(xMax, yMax)$. The calculation of the area of a rectangle results in a specific value that can be expressed by the following equation:

$$amer = (xMax - xMin) * (yMax - yMin) \quad (3)$$

The AMER of the NACA-12XX family airfoils and their corresponding amer areas, as determined by the equation outlined in (3), are illustrated in Figure 5.

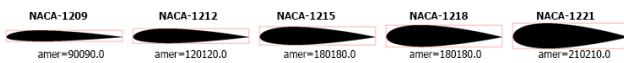


Figure 5. NACA-12XX family airfoils and their AMER areas

2.5. Aspect ratio

The aspect ratio (asr) is a geometric characteristic that can be determined by calculating the ratio of the longer side to the shorter side of the minimum enclosing rectangle bounding the shape [12]. This value can be expressed as

$$asr = \frac{width_{AMER}}{height_{AMER}} \quad (4)$$

where $width_{AMER}$ and $height_{AMER}$ are used to determine the longest and shortest sides of the AMER, respectively. The asr values of the NACA-12XX family of airfoils are shown in Figure 6.



Figure 6. NACA-12XX family airfoils and their aspect ratios

2.6. Circularity

Circularity is a metric used to quantify the degree of roundness, and refers to how closely the shape of an object resembles a perfect circle from a mathematical perspective. This was used to depict the boundary complexity. Circular shapes possess the lowest circularity value of 1.0, and this value progressively increases for more complex shapes, and is computed as follows [16]:

$$cir = \frac{p_s^2}{4\pi a_s} \quad (5)$$

where the area and perimeter of the shape are denoted as a_s and p_s , respectively. Figure 8 presents a summary of the circularity characteristics of airfoils from the NACA-12XX family, calculated using Eq. (5).

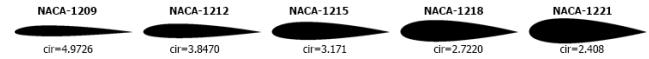


Figure 8. NACA-12XX family airfoils and their circularity values

2.7. Thinness ratio

The thinness ratio is one of the most important shape descriptors and the inverse of the circularity. Regular shapes generally had a higher ratio than irregular shapes. For instance, the maximum value of the thinness for a circle is 1.0. This ratio can be calculated as follows [9].

$$thin = \frac{4\pi a_s}{p_s^2} \quad (6)$$

where a_s and p_s are the perimeter and area of the shape, respectively. In addition, 4π is the normalizing factor. Figure 9 shows the NACA-12XX airfoils and their thinness, calculated using Eq. (6).

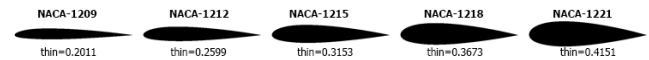


Figure 9. NACA-12XX family airfoils and their thinness values

2.8. Convex hull

The convex hull represents the smallest polygon that encompasses all the contour points of a given shape. [17-26]. In addition, this geometric feature is used to determine the boundaries of a given set of points. For example, the convex hulls of the NACA-55XX airfoils at 1000 points are shown in Figure 10.

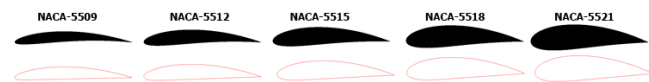


Figure 10. NACA-55XX family airfoils and their convex hulls

Notably, the convex hulls of certain airfoils from the NACA-12XX family follow their perimeters, as illustrated in Figure 11.



Figure 11. NACA-12XX family airfoils and their convex hulls

The significance of the perimeter and area of the convex hull lies in understanding the shapes. As a polygon, the convex hull has n vertices that are enumerated in counterclockwise order. These vertices have the coordinates $(x_1, y_1), (x_2, y_2), \dots, (x_n, y_n)$. The shoelace formula can be employed to determine the polygon area as follows [27]:

$$c = \frac{1}{2} \sum_{i=1}^n x_i y_{i+1} - x_{i+1} y_i \quad (7)$$

where c is the area of the convex hull and x_i and y_i are the coordinates of the vertices. The convex hull areas of the NACA-55XX and NACA-12XX family airfoils were calculated using Eq. (7), are shown in Figures 12a and 12b, respectively.

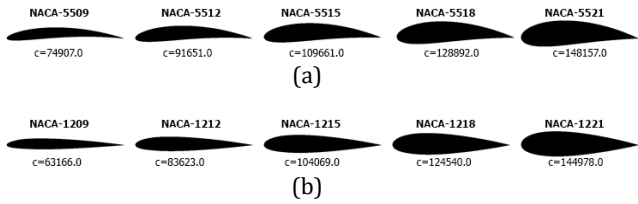


Figure 12. Areas of Convex Hull for a)NACA-55XX b)NACA-12XX

As illustrated in Figure 12b, the convex areas of the NACA-12XX airfoils are nearly equal to their areas of curvature. This is because the convex hull of each airfoil closely resembled its contour.

The calculation of the convex hull's perimeter involves summing the Euclidean distances between its vertices. A mathematical formula exists to determine this perimeter, which can be expressed as follows:

$$h = \frac{1}{2} \sum_{i=1}^n \sqrt{(x_{i+1} - x_i)^2 + (y_{i+1} - y_i)^2} \quad (8)$$

where the perimeter of the convex hull is denoted by h and its vertex coordinates are represented by x_i and y_i , respectively. The perimeters of the convex hulls of the NACA-55XX and NACA-12XX airfoil families were determined using Eq. (8) are shown in Figures 13a and 13b, respectively.

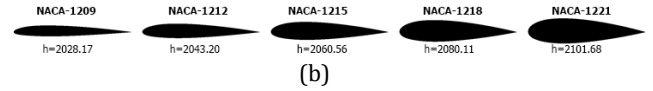
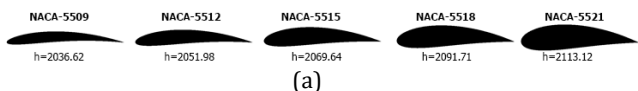


Figure 13. Perimeters of Convex Hull a)NACA-55XX b) NACA-12XX

The convex hull perimeters of the NACA-12XX family are almost identical to their perimeters, as shown in Figure 13b. This is due to the fact that the convex hull closely follows the contour of each airfoil.

2.9. Contour temperature

The concept of contour temperature is rooted in a well-established thermodynamic framework, as proposed by the authors who first introduced this concept [27]. According to their hypothesis, a strong correlation exists between the contour temperature and fractal dimension. This feature is defined as follows:

$$t = (\log_2(\frac{2p}{p-h}))^{-1} \quad (9)$$

where t is the contour temperature, p is the perimeter of the shape, and h is the perimeter of the convex hull. The airfoils of NACA-55XX and NACA-12XX are shown in Figure 15a and 15b, respectively.

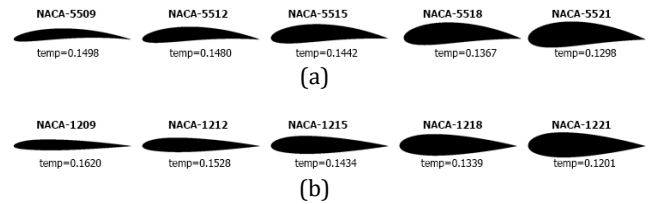


Figure 15. Contour Temperature of Airfoils a)NACA-55XX b) NACA-12XX

3. Airfoil dataset

To demonstrate the effectiveness of the methods presented, we evaluated 120 airfoils from four NACA families, as shown in Figure 17 (Appendix A). All airfoils had 1000 points and each NACA family member had 30 airfoils. In addition, the same suffix is used for airfoil families, such as 0K09, 2K12, 4K15, and 6K18, where K={2,3,4,5,6,7}.

The ImageJ platform was used to calculate the simple shape descriptors. As open-source software for processing and analyzing scientific images, it offers a wide range of capabilities, including various extensions and related software projects.

4. Results and Discussion

Table 1 in Appendix B. presents a summary of the outcomes from the preliminary examination of the nine distinct shape characteristics using the airfoil dataset depicted in Figure 17.

The last two digits of an airfoil's designation signify the maximum thickness of the airfoil as a percentage of chord length. As these digits became larger, both the area and perimeter of the airfoil increased. As shown in Table 1, airfoils from all NACA families experienced an increase in both area and perimeter. In addition, the apr ratio increased in every NACA family member.

The dimensions of the minimum enclosing rectangle demonstrate a linear correlation with the enclosed area. As a result, enlargement of the shape area led to a corresponding increase in the size of the MER. The connection between the two variables was apparent from the increasing trend of the amr values, as shown in Table 1. As asr ratio of an airfoil is related to its width and height, it follows that the values of these dimensions increase with the thickness of the airfoil.

An inverse relationship was observed between circularity and thickness of the airfoils. The circularity and thinness values converged towards 1.0 as the airfoil thickness increased. Table 1 illustrates this phenomenon, demonstrating that for each airfoil, circularity approached 1.0 with increasing thickness, whereas thinness concurrently decreased, approaching 1.0.

As shown in Table 1, the area and perimeter of the convex hull exhibited a high degree of correlation with the area of the airfoil for symmetrical and near-symmetrical families, specifically 0YYY and 2YYY. However, for less symmetrical airfoils, the results obtained from the convex hull area and perimeter were less accurate, with greater discrepancies present in relation to the airfoil area and perimeter, such as 4YYY and 6YYY. In addition, the convex area and perimeter increased with the thickness ratio for all the airfoil families. Because not all airfoils were irregular in shape, the solidity values produced outcomes close to 1.0. Furthermore, the solidity slightly increased with increasing thickness. The temperature and thickness of the contour were found to be inversely proportional, with a decrease in temperature corresponding to an increase in thickness. Furthermore, the temperatures of the airfoils for the same suffix in a family were very similar, such as the NACA-0209 and NACA-0309 airfoils.

4.1. Correlation of shape descriptors with drag coefficient

In the configuration of the airfoil, parameters such as the maximum thickness, maximum camber, and leading-edge radius play a crucial role in the aerodynamic performance. For the NACA family, the effects of specific parameters on aircraft design were documented in Raymer's textbook [4]. Figure 16 shows that the drag coefficient increased proportionally with the thickness ratio. When the shape parameters were analyzed (Table 1) for the NACA 24XX family, it was observed that while the

aspect ratio (asr), circularity (circ), and temperature (t) were inversely related to the drag coefficient as the thickness increased, the other parameters were directly proportional to the drag coefficient.

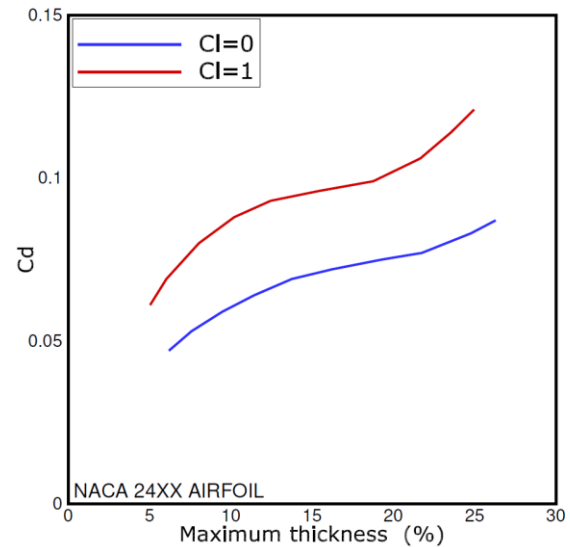


Figure 16. Effect of thickness on drag [4].

5. Conclusions

The primary objective of this study was to investigate the shape of airfoils by using simple shape descriptors. One of the most significant findings of this study is that an increase in the thickness of the airfoil results in a corresponding increase in its area, perimeter, AMER area, and convex hull area. Another significant observation is that the values derived from these basic features either increased or decreased. However, these shape properties are not utilized independently, because they do not possess unique attributes that distinguish them from one another. There is a correlation with aerodynamic design parameters, such as drag, for shape descriptors, and this correlation should be investigated in more detail. The combination of these features with other shape attributes, such as chain code histograms, shape signatures, and central moments, can enhance the success of machine learning and deep learning applications. For instance, these features can be utilized in aerodynamic applications to estimate aerodynamic loads, such as Cl and Cd.

Declaration of Ethical Code

In this study, we assume that all the rules required to be followed within the scope of the "Higher Education Institutions Scientific Research and Publication Ethics Directive" are complied with, and that none of the actions stated under the heading "Actions Against Scientific Research and Publication Ethics" are not carried out.

References

- [1] Santos, M., Mattos, B., Girardi, R. 2008. Aerodynamic coefficient prediction of airfoils using neural networks. 46th AIAA aerospace sciences meeting and exhibit. P.887.
- [2] Du, X., He, P., Martins, J.R. 2021. Rapid airfoil design optimization via neural networks-based parameterization and surrogate modeling. *Aerospace Science and Technology* 113.106701.
- [3] Chen, H., He, L., Qian W., Wang, S. 2020. Multiple aerodynamic coefficient prediction of airfoils using a convolutional neural network. *Symmetry*. 12(4) 544.
- [4] Raymer, D. 2012. Aircraft design: a conceptual approach. American institute of aeronautics and astronautics.
- [5] Birajdar, M.R., Kale, S.A. 2015. Effect of leading edge radius and blending distance from leading edge on the aerodynamic performance of small wind turbine blade airfoils. *International journal of energy and power engineering*. 4 (5-1)54-58.
- [6] Lim, J.W. 2018. Application of parametric airfoil design for rotor performance improvement. <https://dspaceerf.nlr.nl/server/api/core/bitstreams/d428da1f-ca7a-4baf-93090924a609721e/content> (Erişim Tarihi: 14.10.2024).
- [7] Santos, M., Mattos, B., & Girardi, R. 2008, January. Aerodynamic coefficient prediction of airfoils using neural networks. In *46th AIAA aerospace sciences meeting and exhibit* (p. 887).
- [8] Zhang, Y., Sung, W. J., & Mavris, D. N. 2018. Application of convolutional neural network to predict airfoil lift coefficient. In *2018 AIAA/ASCE/AHS/ASC structures, structural dynamics, and materials conference* (p. 1903).
- [9] Da Fona Costa, F., Jr. Cesar, R.M. 2018. Shape classification and analysis: theory and practice. Crc Press.
- [10] Freeman, H. 1961. On the encoding of arbitrary geometric configurations. *IRE transactions on electronic computers*. (2) 260-268.
- [11] Gonzales, R., Woods, R. 2018. Digital image processing. Pearson.
- [12] Castleman, K. 1996. Digital image processing. Prentice Hall.
- [13] Freeman, H., Shapira R. 1975. Determining the minimum-area encasing rectangle for an arbitrary closed area curve. *Commun. ACM* 18 (7) 409-413.
- [14] Toussaint G.T. 1983. Solving geometric problems with rotating calipers. *Proc. IEEE Melecon*. Vol.83 p.A10.
- [15] Toussaint G.T. 2014. The rotating calipers: An efficient, multipurpose, computational tool. The international conference on computing technology and information management (ICCTIM). P215.
- [16] Merchant, F., Castleman, K. 2022. Microscope image processing. Academic press.
- [17] Chand, D.R., Kapur, S.S. 1970. An algorithm for convex polytopes. *Journal of the ACM (JACM)*. 17(1) 78-86.
- [18] Jarvis, R.A. 1973. On the identification of the convex hull of a finite set of points in the plane. *Information processing letters* 2(1) 18-21.
- [19] Graham, R.L. 1972. An efficient algorithm for determining the convex hull of a finite planar set. *Info. Proc. Lett.* 1 132-133.
- [20] Eddy, W.F. 1977. A new convex hull algorithm for planar sets, *ACM transactions on mathematical software (TOMS)*. 3 (4) 398-403.
- [21] Bykat, A. 1978. Convex hull of a finite set of points in two dimensions. *Information processing letters*. 7(6) 296-298.
- [22] Preparata, F.P., Hong, S.J. 1977. Convex hulls of finite sets of points in two and three dimensions. *Communications of the ACM*. 20(2) 87-93.
- [23] Andrew, A.M. 1979. Another efficient algorithm for convex hulls in two dimensions. *Information processing letters*. 9(5) 216-219.
- [24] Kallay, M. 1984. The complexity of incremental convex hull algorithms in rd. *Information processing letters*. 19(4) 197.
- [25] Kirkpatrick, D.G., Seidel, R. 1986. The ultimate planar convex hull algorithm? . *SIAM journal on computing*. 15(1) 287-299.
- [26] Chan, T.M. 1996. Optimal output-sensitive convex hull algorithms in two and three dimensions. *Discrete & computational geometry*. 16(4) 361-368.
- [27] Dupain, Y., Kamae, T., Mendes, M. 1986. Can one measure the temperature of a curve?. *Archive for rotational mechanics and analysis*. 94 155-163.

Appendix A.

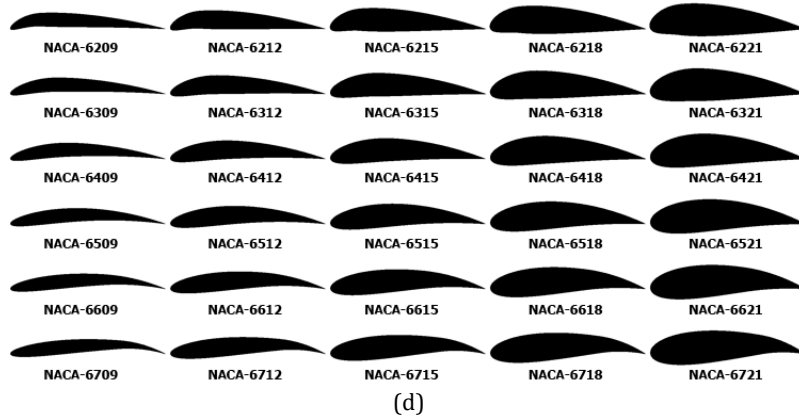
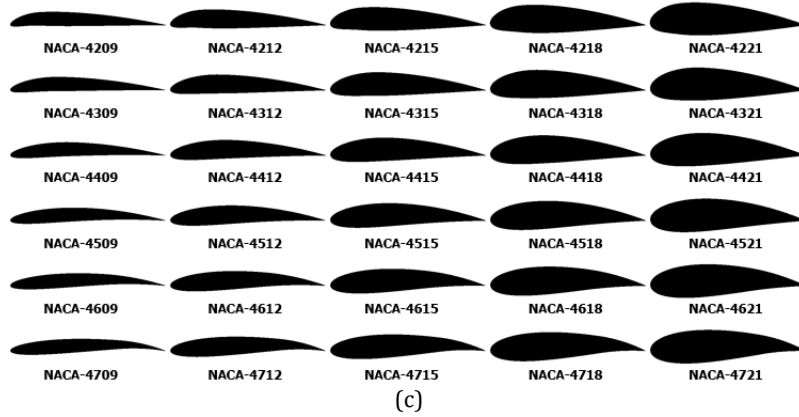
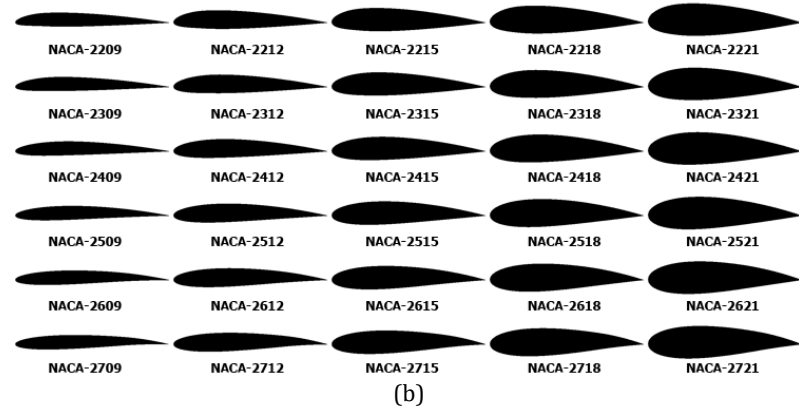
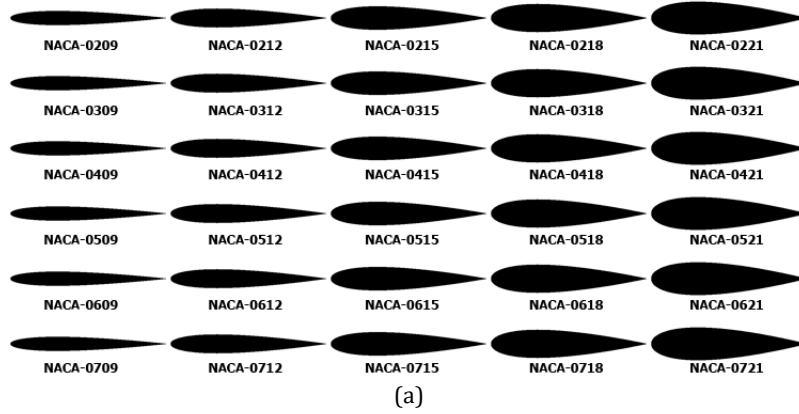


Figure 17. Airfoil Families a)NACA-0YYY b) NACA-2YYY c)NACA-4YYY d)NACA-6YYY

Appendix B.**Table 1.** Results for shape parameters of NACA-XXXX airfoils

Airfoils	a	p	apr	amer	asr	cir	Thin	c	t
NACA-0209	62273	1973,46	31,56	91000	10,9890	4,9768	0,2009	63203	0,1614
NACA-0212	82725	2000,32	41,36	121000	8,2645	3,8490	0,2598	83649	0,1520
NACA-0215	103159	2028,28	50,86	151000	6,6225	3,1735	0,3151	104076	0,1426
NACA-0218	123609	2056,25	60,11	181000	5,5249	2,7220	0,3674	124506	0,1337
NACA-0221	144055	2088,67	68,97	211000	4,7393	2,4099	0,4150	144960	0,1189
NACA-0309	62273	1973,46	31,56	91000	10,9890	4,9768	0,2009	63203	0,1614
NACA-0312	82725	2000,32	41,36	121000	8,2645	3,8490	0,2598	83649	0,1520
NACA-0315	103159	2028,28	50,86	151000	6,6225	3,1735	0,3151	104076	0,1426
NACA-0318	123609	2056,25	60,11	181000	5,5249	2,7220	0,3674	124506	0,1337
NACA-0321	144055	2088,67	68,97	211000	4,7393	2,4099	0,4150	144960	0,1189
NACA-0409	62273	1973,46	31,56	91000	10,9890	4,9768	0,2009	63203	0,1614
NACA-0412	82725	2000,32	41,36	121000	8,2645	3,8490	0,2598	83649	0,1520
NACA-0415	103159	2028,28	50,86	151000	6,6225	3,1735	0,3151	104076	0,1426
NACA-0418	123609	2056,25	60,11	181000	5,5249	2,7220	0,3674	124506	0,1337
NACA-0421	144055	2088,67	68,97	211000	4,7393	2,4099	0,4150	144960	0,1189
NACA-0509	62273	1973,46	31,56	91000	10,9890	4,9768	0,2009	63203	0,1614
NACA-0512	82725	2000,32	41,36	121000	8,2645	3,8490	0,2598	83649	0,1520
NACA-0515	103159	2028,28	50,86	151000	6,6225	3,1735	0,3151	104076	0,1426
NACA-0518	123609	2056,25	60,11	181000	5,5249	2,7220	0,3674	124506	0,1337
NACA-0521	144055	2088,67	68,97	211000	4,7393	2,4099	0,4150	144960	0,1189
NACA-0609	62273	1973,46	31,56	91000	10,9890	4,9768	0,2009	63203	0,1614
NACA-0612	82725	2000,32	41,36	121000	8,2645	3,8490	0,2598	83649	0,1520
NACA-0615	103159	2028,28	50,86	151000	6,6225	3,1735	0,3151	104076	0,1426
NACA-0618	123609	2056,25	60,11	181000	5,5249	2,7220	0,3674	124506	0,1337
NACA-0621	144055	2088,67	68,97	211000	4,7393	2,4099	0,4150	144960	0,1189
NACA-0709	62273	1973,46	31,56	91000	10,9890	4,9768	0,2009	63203	0,1614
NACA-0712	82725	2000,32	41,36	121000	8,2645	3,8490	0,2598	83649	0,1520
NACA-0715	103159	2028,28	50,86	151000	6,6225	3,1735	0,3151	104076	0,1426
NACA-0718	123609	2056,25	60,11	181000	5,5249	2,7220	0,3674	124506	0,1337
NACA-0721	144055	2088,67	68,97	211000	4,7393	2,4099	0,4150	144960	0,1189
NACA-2209	62410	1973,46	31,62	90090	11,1222	4,9658	0,2014	63265	0,1636
NACA-2212	82866	2000,32	41,43	120120	8,3417	3,8425	0,2602	83706	0,1544
NACA-2215	103329	2028,28	50,94	150150	6,6733	3,1683	0,3156	104180	0,1453
NACA-2218	123789	2057,92	60,15	180180	5,5611	2,7225	0,3673	124654	0,1351
NACA-2221	144245	2087,00	69,12	210210	4,7667	2,4029	0,4162	145107	0,1255
NACA-2309	62397	1973,69	31,61	91091	11,0000	4,9680	0,2013	63282	0,1629
NACA-2312	82810	2001,10	41,38	121121	8,2727	3,8481	0,2599	83743	0,1534
NACA-2315	103274	2029,07	50,90	151151	6,6291	3,1724	0,3152	104212	0,1441
NACA-2318	123729	2058,15	60,12	181181	5,5304	2,7244	0,3671	124672	0,1342
NACA-2321	144195	2087,78	69,07	211211	4,7441	2,4055	0,4157	145128	0,1237
NACA-2409	62372	1975,81	31,57	93093	11,0013	4,9807	0,2008	63287	0,1613
NACA-2412	82862	2001,88	41,39	122122	8,2632	3,8487	0,2598	83749	0,1527
NACA-2415	103287	2029,85	50,88	152152	6,6294	3,1745	0,3150	104192	0,1431
NACA-2418	123731	2058,15	60,12	181181	5,5556	2,7244	0,3671	124607	0,1340

NACA-2421	144193	2087,78	69,07	211211	4,7391	2,4056	0,4157	145094	0,1235
NACA-2509	62360	1975,81	31,56	93093	10,9898	4,9817	0,2007	63922	0,1612
NACA-2512	82823	2001,88	41,37	122122	8,2548	3,8505	0,2597	83768	0,1526
NACA-2515	103290	2029,30	50,90	152152	6,6227	3,1727	0,3152	104159	0,1436
NACA-2518	123730	2058,38	60,11	182182	5,5190	2,7250	0,3670	124606	0,1337
NACA-2521	144178	2086,67	69,09	211211	4,7622	2,4033	0,4161	145049	0,1249
NACA-2609	62366	1975,81	31,56	93093	10,9906	4,9812	0,2008	64901	0,1612
NACA-2612	82817	2002,11	41,36	123123	8,2551	3,8517	0,2596	84662	0,1523
NACA-2615	103248	2029,85	50,86	152152	6,6221	3,1757	0,3149	104623	0,1433
NACA-2618	123713	2057,59	60,13	181181	5,5192	2,7233	0,3672	124809	0,1348
NACA-2621	144168	2087,78	69,05	211211	4,7566	2,4060	0,4156	145101	0,1236
NACA-2709	62384	1973,36	31,61	93000	10,9780	4,9674	0,2013	65433	0,1613
NACA-2712	82810	2001,88	41,37	122122	8,2644	3,8511	0,2597	85484	0,1527
NACA-2715	103291	2029,30	50,90	152152	6,6662	3,1726	0,3152	105498	0,1439
NACA-2718	123747	2058,93	60,10	182182	5,5248	2,7261	0,3668	125662	0,1336
NACA-2721	144171	2088,57	69,03	212212	4,7615	2,4077	0,4153	145873	0,1229
NACA-4209	62632	1980,84	31,62	94094	10,7632	4,9853	0,2006	64586	0,1644
NACA-4212	83135	2004,66	41,47	120240	8,3500	3,8467	0,2600	84221	0,1578
NACA-4215	103690	2032,40	51,02	150300	6,6800	3,1701	0,3154	104640	0,1492
NACA-4218	124241	2062,82	60,23	180540	5,5722	2,7255	0,3669	125126	0,1388
NACA-4221	144775	2095,47	69,09	210840	4,7810	2,4136	0,4143	145676	0,1255
NACA-4309	62499	1979,18	31,58	99000	10,4053	4,9875	0,2005	66202	0,1623
NACA-4312	83068	2004,56	41,44	124124	8,2728	3,8494	0,2598	84199	0,1561
NACA-4315	103606	2030,96	51,01	152152	6,6288	3,1682	0,3156	104533	0,1484
NACA-4318	124149	2060,04	60,27	181362	5,5359	2,7202	0,3676	125069	0,1394
NACA-4321	144644	2090,24	69,20	211422	4,7488	2,4037	0,4160	145589	0,1294
NACA-4409	62534	1983,32	31,53	102000	10,3091	5,0057	0,1998	68424	0,1585
NACA-4412	83019	2006,36	41,38	127127	8,1305	3,8586	0,2592	85982	0,1538
NACA-4415	103537	2032,76	50,93	155155	6,6171	3,1759	0,3149	104821	0,1460
NACA-4418	124079	2061,06	60,20	184184	5,5437	2,7244	0,3671	125016	0,1374
NACA-4421	144573	2090,46	69,16	213213	4,7294	2,4054	0,4157	145468	0,1279
NACA-4509	62507	1985,68	31,48	102000	10,3101	5,0197	0,1992	70085	0,1562
NACA-4512	83039	2006,03	41,39	129000	8,1882	3,8564	0,2593	87871	0,1520
NACA-4515	103522	2033,77	50,90	157157	6,6091	3,1795	0,3145	107027	0,1449
NACA-4518	124030	2062,62	60,13	186186	5,5330	2,7296	0,3664	126439	0,1356
NACA-4521	144528	2092,59	69,07	215215	4,7483	2,4110	0,4148	146279	0,1250
NACA-4609	62495	1989,04	31,42	102000	10,4182	5,0377	0,1985	71516	0,1535
NACA-4612	83003	2008,61	41,32	129000	8,1788	3,8680	0,2585	89653	0,1497
NACA-4615	103482	2031,88	50,93	157000	6,6394	3,1748	0,3150	108575	0,1446
NACA-4618	124008	2062,62	60,12	186186	5,5039	2,7301	0,3663	128388	0,1357
NACA-4621	144499	2090,92	69,11	215215	4,7204	2,4077	0,4153	148084	0,1275
NACA-4709	62480	1992,18	31,36	101000	10,6407	5,0548	0,1978	72686	0,1513
NACA-4712	82952	2013,32	41,20	129000	8,1803	3,8885	0,2572	91128	0,1460
NACA-4715	103457	2035,80	50,82	157000	6,6398	3,1879	0,3137	110201	0,1414
NACA-4718	123949	2062,85	60,09	186000	5,4971	2,7320	0,3660	129717	0,1335
NACA-4721	144453	2090,14	69,11	215000	4,7157	2,4066	0,4155	149463	0,1265
NACA-6209	62992	2005,25	31,41	110110	9,1833	5,0797	0,1969	75409	0,1543
NACA-6212	83620	2015,74	41,48	129129	7,8735	3,8668	0,2586	88130	0,1577

NACA-6215	104306	2044,24	51,02	151604	6,6490	3,1882	0,3137	105864	0,1507
NACA-6218	124996	2070,74	60,36	181905	5,5525	2,7299	0,3663	126185	0,1443
NACA-6221	145635	2101,71	69,29	212266	4,7678	2,4136	0,4143	146678	0,1341
NACA-6309	62819	2003,25	31,36	114000	8,9286	5,0836	0,1967	76944	0,1517
NACA-6312	83437	2017,66	41,35	136136	7,5836	3,8827	0,2576	91300	0,1527
NACA-6315	104110	2040,24	51,03	160320	6,4645	3,1817	0,3143	107251	0,1501
NACA-6318	124733	2067,30	60,34	185555	5,5049	2,7266	0,3668	126062	0,1430
NACA-6321	145356	2097,04	69,31	212848	4,7535	2,4075	0,4154	146322	0,1342
NACA-6409	62767	2006,62	31,28	115000	8,9993	5,1049	0,1959	78509	0,1468
NACA-6412	83422	2021,26	41,27	139000	7,4628	3,8972	0,2566	93990	0,1475
NACA-6415	103995	2040,37	50,97	164000	6,3625	3,1856	0,3139	110538	0,1459
NACA-6418	124621	2068,44	60,25	191382	5,4895	2,7320	0,3660	128665	0,1401
NACA-6421	145198	2098,73	69,18	219438	4,7469	2,4140	0,4142	147420	0,1301
NACA-6509	62784	2009,98	31,24	116000	9,0087	5,1206	0,1953	80129	0,1426
NACA-6512	83324	2026,74	41,11	140000	7,5198	3,9230	0,2549	96232	0,1414
NACA-6515	103901	2045,53	50,79	167000	6,3582	3,2047	0,3120	113490	0,1402
NACA-6518	124484	2068,11	60,19	193000	5,4430	2,7342	0,3657	131604	0,1370
NACA-6521	145087	2098,08	69,15	221442	4,7213	2,4144	0,4142	150846	0,1301
NACA-6609	62712	2013,90	31,14	115000	9,1744	5,1465	0,1943	81319	0,1384
NACA-6612	83253	2029,55	41,02	139000	7,6243	3,9372	0,2540	98046	0,1382
NACA-6615	103811	2049,68	50,65	166000	6,4376	3,2205	0,3105	115710	0,1356
NACA-6618	124421	2072,49	60,03	194000	5,4730	2,7471	0,3640	134232	0,1322
NACA-6621	145020	2095,85	69,19	221000	4,7071	2,4104	0,4149	153199	0,1299
NACA-6709	62673	2017,82	31,06	114000	9,3464	5,1698	0,1934	82549	0,1352
NACA-6712	83272	2035,04	40,92	139000	7,7434	3,9576	0,2527	99708	0,1333
NACA-6715	103784	2055,17	50,50	165000	6,4809	3,2386	0,3088	117679	0,1304
NACA-6718	124360	2078,30	59,84	192000	5,4678	2,7639	0,3618	136322	0,1261
NACA-6721	144956	2102,91	68,93	221000	4,7252	2,4277	0,4119	155495	0,1217